Environmental Research Communications

CrossMark

PAPER

Behavior of polypyrrole-coated cotton fabric undergoing biodegradation in compost-enriched soil

Marta Piccioni [ORCID] , Alessio Varesano [ORCID] and Maria Laura Tummino [ORCID]

CNR-STIIMA, National Research Council—Institute of Intelligent Industrial Technologies and Systems for Advanced Manufacturing, Corso Giuseppe Pella 16, 13900 Biella, Italy

E-mail: marialaura.tummino@cnr.it

Abstract

This study investigated the biodegradation behavior of cotton fabrics treated with polypyrrole, a polymer with conductive and antibacterial properties. Fabric samples were buried in compost-enriched soil for 10, 30 and 90 days. The biodegradation level was initially estimated by a visual inspection of the fibers and by the determination of the fabric weight loss. Other physical–chemical changes of fibers during the biodegradation process were analyzed by microscopy, thermal analyses and infrared spectroscopy. The surface resistivity of the fabrics was also measured. The results obtained comparing the bare cotton samples and the polypyrrole-added ones suggested that, on the one hand, polypyrrole hindered/delayed the biodegradation of cotton in compost-enriched soil, probably exercising its inherent antimicrobial feature during the first period of burial. On the other hand, over time, polypyrrole seemed to represent the first compound attacked by the microorganisms, preserving the cotton substrate. Despite the absence of dedicated literature regarding polypyrrole biodegradation, the mechanism hypothesized in this paper involves the loss of conjugation, as a consequence of de-doping, oxidized functionalities up to local cycle breaking.

1. Introduction

In the last years, the serious issue of textile waste accumulation has raised attention all over the world. The clothing industry is one of the most polluting industries, producing more than 92 million tons of textile in 2013 and it is expected that fashion waste will reach about 148 million tons by 2030 [1–3].

This negative aspect in the next years will tend to increase because of the continuing trends in fast fashion fueled by growing global consumerism, wealth and population [4]. In fact, the fast fashion phenomenon involves a reduced garment usage time before it is discarded due to quick style changes and low quality/price [5, 6].

One of the parameters to take into account to evaluate the sustainability of textile products is, for instance, their biodegradability and this is true for conventional cloths, but also for advanced materials, such as smart textiles [7]. Biodegradation routes can imply anaerobic or aerobic digestion, or landfilling to pass from large or complex molecules to simple, small, and nontoxic compounds, as a consequence of various microorganisms' activity [7]. These actions involve various stages, namely (i) bio-deterioration (the combined intervention of microbial communities and abiotic factors to break the materials into fragments), (ii) depolymerization (operated by microorganisms' secreted enzymes and free radicals capable of polymer cleavage), (iii) assimilation into the plasma membrane of the biological agent and, finally, (iv) mineralization [8].

Many studies are focused on the biodegradation of polymers like polyethylene, polyethylene terephthalate, etc or bio-based polymers in different environments (soil, seawater, etc) and different microorganisms and enzymes have been identified [9–12]. Egan *et al* [4] reported and listed some of the enzymes capable of catalyzing the depolymerization of common textile polymers in the primary degradation steps (and the related products). These enzymes were protease for silk, wool, polylactic acid, and polyamides, cutinase for polyesters and nitrilase

for polyacrylonitrile, to give some examples. In real conditions, the primary degradation is also influenced by environmental abiotic factors such as heat, UV radiation, oxygen, water, mechanical stress, pH, etc [13].

Synthetic fibers, often from a petrochemical origin, represent a large part of the global textile market (around 64% by volume), producing 111 million metric tons of fiber annually [4]. Especially due to their hydrophobic and crystalline features, these polymers are generally recalcitrant to biodegradation [14], taking 30 to 40 years to break and another hundred years to decay completely [15]. Nevertheless, Wang *et al* [9], for instance, subjected films of polyamide 4 to biodegradation in four types of soils. The results showed that the highest degradation occurred in composted soil in 60 days since almost no residual films were observed therein with respect to other soil types. PA4 degradation was promoted by bacteria such as *Ensifer* and *Luteimonas*, which play a key role in nitrogen fixation.

On the contrary, natural fibers, which come from plants or animals, are renewable thanks to their biological origin and exhibit biodegradability in their natural forms, taking weeks to years to disintegrate in a landfill [4, 15]. In particular, cotton, the most widely used natural fiber available, is composed of cellulose, a biodegradable polymer that consists of glucose monomers linked together by β-glycosidic linkages [16, 17].

The biodegradation process causes depolymerization of the cellulose macromolecules, which is translated into a decreased molecular weight and strength, increased solubility and changed crystallinity [18, 19]. This depolymerization is initiated by microorganisms present in soil, water and air, that cause the hydrolytic and oxidative degradation of cellulose [18, 19]. The secreted enzymes, called cellulases, promote the break of biologically created chemical bonds and modify the chemistry of cellulose [4, 16]. These enzymes can be divided into endoglucanases, which are capable of hydrolyzing the $\beta-1$, 4-glycosidic linkages present in amorphous cellulose, and cellobiohydrolases that can react with the end groups of cellulose [16].

Fungi and bacteria represent the major source of cellulolytic enzymes, but act in two different modes to degrade cotton fabrics. Fungi belonging to the genera *Alternaria* sp., *Trichoderma* sp. [20], *Penicillium* sp. and *Aspergillus* sp., attack fibers from the inside towards the outer layer of fibers. On the contrary, *Bacillus* sp. and *Clostridium* sp. proceed from the cotton fiber surface towards the inner parts and make more effort to carry out the process because they need a higher percentage of moisture, which requires the fabric to be saturated throughout the whole process of degradation [19].
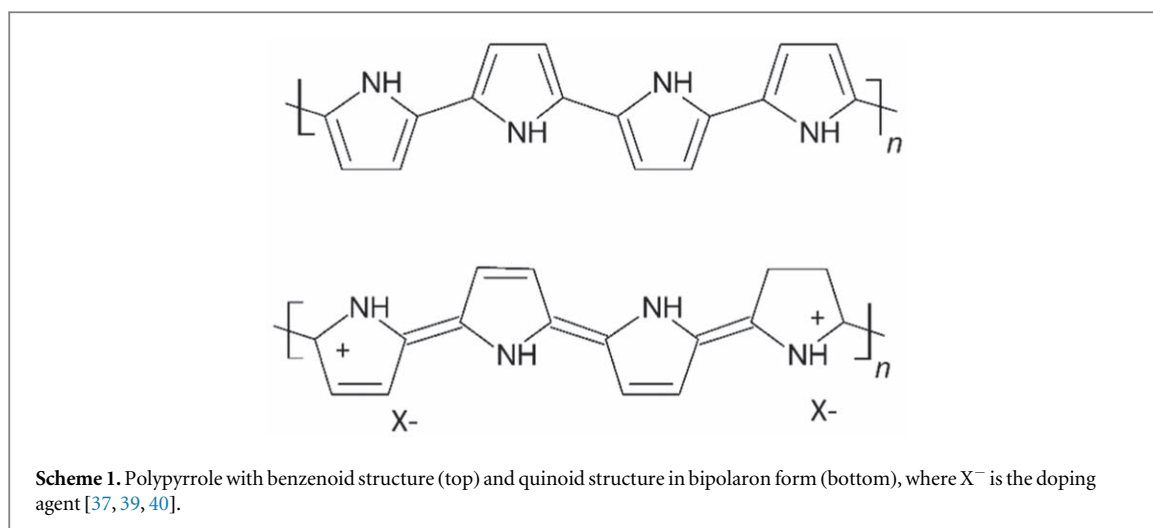
Complete biodegradation of cellulose under aerobic conditions results in carbon dioxide and water and, under anaerobic conditions, in carbon dioxide, methane and water, which present no harm to the environment [16, 21]. Besides the type of microorganism considered, also the type of environment (natural, man-made environments) is a variable factor that can influence the biopolymer's degradation mechanism [16]. Depending on the soil type, a 10-week period of keeping cellulose in soils led to 82%–95% degradation [22].

On the other hand, fabrics and textile materials are widely used in geotechnical engineering [23–26] and agriculture [27] because they are cheap, light and easy to install. In geotechnical engineering, they are called geotextiles. The requirements for long-term applications include a low biodegradability in soil. Most geotextiles consist of synthetic polymers [24, 26], such as polyolefins, polyesters and polyamides. However, when natural fibers [23, 26, 28] or biopolymers [24, 26] are used, additives can be added to improve their stability [29]. The additives can include coatings of bitumen [30, 31], for instance. In the soil, synthetic polymers may degrade into small particles (i.e., microplastics) by mechanical and chemical actions and additives can be leached, causing potential adverse effects to the environment [24].

One of the most utilized and suitable polymers for deposition on textile and geotextile materials is polypyrrole (PPy), a nitrogen-containing polymer obtained by chemical oxidative polymerization of the monomer pyrrole [32], because it is easy to synthesize, possesses good stability and it is a conductive polymer [33–36], thanks to its extended π-conjugated backbone long chain [37]. Along the PPy chain, positive charges can be introduced, which are counter-balanced by anionic counter-ions (dopants or doping agents), such as sulfonates [38] (scheme 1). In detail, according to [39], during doping, PPy is oxidized and a π-electron is removed from the neutral PPy chain, changing its structure from the benzenoid structure (aromatic) to a quinoid form. Subsequently, a polaron is formed, and with further oxidation, a second electron is eliminated from the PPy chain, leading to the formation of a doubly charged bipolaron. PPy can be, therefore, considered an ionic complex consisting of cations and embedded counter-ions. Moreover, due to the presence of these positive charges, polypyrrole exercises good antibacterial properties against both Gram-positive and Gram-negative bacteria on textiles [41].

Polypyrrole has often been taken into account as a suitable compound for biodegradable systems, although no specific studies, to the best of the author's knowledge, have been devoted to the biodegradation pathways of polypyrrole [33, 42–47].

In the present work, cotton fibers were treated with polypyrrole and buried in a controlled lab soil environment. Using the untreated cotton samples as a control, this study aimed to investigate the behavior of cotton fibers treated with PPy over time in order to understand if this type of treatment promoted or delayed the natural biodegradation process of cotton in soil. Untreated cotton and treated cotton samples were taken from

Scheme 1. Polypyrrole with benzenoid structure (top) and quinoid structure in bipolaron form (bottom), where X^- is the doping agent [37, 39, 40].

the compost-enriched soil after 10, 30 and 90 days. Physical–chemical changes after different periods of biodegradation were determined from electron microscopic, thermal and spectroscopic analyses, in addition to surface resistivity measurements.

2. Materials and methods

2.1. Materials

A cotton fabric (plain weave fabric suitable for ISO 105-F02, mass per unit area 110.75 g m^{-2} determined in accordance with ISO 3801, supplied by Testfabrics Inc., West Pittston, PA, USA) was used as the textile substrate for polypyrrole deposition and as a reference sample.

Chemicals used for the synthesis of PPy were pyrrole 97% by Fluka (Germany), dicyclohexyl sulfosuccinate sodium salt (DSS) by Fluka (Germany) and ferric chloride hexahydrate by Sigma-Aldrich (Germany).

The media used for evaluating the biodegradation of fabrics was a compost-enriched soil (COMPO Italia Srl, Cesano Maderno MB, Italy). It is composed of neutral sphagnum, composted green soil improver and pumice and it contains mineral fertilizer and guano. The pH(H_2O) of the soil was measured as 7, the apparent density in dry form is declared as 250 kg m^{-3} and the total porosity is 87.5% v/v.

2.2. PPy coating on cotton fabric

PPy deposition was carried out at room temperature by plunging the fabrics in a stirred ferric chloride and DSS solution. After impregnation of 10 min, the monomer pyrrole (4 g L^{-1}) was drop-wise added to the solution, which became dark because of PPy production. Cotton fabrics were pulled out from the polymerization bath after 4 h and dried at room temperature. A detailed procedure was reported in [38].

2.3. Soil burial test

Four beakers were filled with a total volume of ca. 1600 cm^3 of compost-enriched soil. Two of the four beakers were placed in an oven at 105 °C for 24 h to obtain a reference sterilized soil (without active microorganisms) [48]. The other two containers, covered with aluminum foils, were left under the fume hood. In the meantime, the cotton and PPy-cotton samples were cut into a total of 12 pieces of about 4 cm^2. Table 1 reports the sample labels.

Three untreated cotton samples were put into the beaker containing the sterilized soil and three untreated cotton samples were put into the beaker containing non-sterile soil. The same subdivision was done for the six PPy-treated cotton samples in the other two soils (sterilized and non-sterile). Each fabric piece was buried about 3 cm deep from the surface and an identification flag was placed on the right of it to find and take the sample more easily after the burial. Then, all the beakers were covered with aluminum foils. The samples were withdrawn from the compost-enriched soil after 10, 30 and 90 days. All the soils were moistened every three days with 10 ml of distilled water to avoid complete dryness. All the experiments were conducted in a conditioned laboratory at 20 °C and 65% RH (relative humidity).

2.4. Characterization

After a gentle removal of excess soil matter from the samples, the fabrics were weighed before and after the biodegradation process and were characterized with SEM, TGA, DSC, FTIR and electrical measurements.

Table 1. Sample labels for each formulation/ biodegradation treatment.

Sample	Composition	Days of burial	Type of soil
Cotton	Standard Cotton	—	—
Cotton-PPy	Cotton + PPy	—	—
A	Cotton	10	Non-sterile
B	Cotton	30	Non-sterile
C	Cotton	90	Non-sterile
A(P)	Cotton + PPy	10	Non-sterile
B(P)	Cotton + PPy	30	Non-sterile
C(P)	Cotton + PPy	90	Non-sterile
D	Cotton	10	Sterilized
E	Cotton	30	Sterilized
F	Cotton	90	Sterilized
D(P)	Cotton + PPy	10	Sterilized
E(P)	Cotton + PPy	30	Sterilized
F(P)	Cotton + PPy	90	Sterilized

Morphological investigations were performed using an EVO 10 Scanning Electron Microscope (SEM, Carl Zeiss AG, Oberkochen, Germany) with an acceleration voltage of 20 kV. The samples were sputter-coated with a 20 nm-thick gold layer in rarefied argon, using a Quorum Q150R ES Plus Sputter Coater.

For Thermogravimetric Analyses (TGA, Mettler Toledo TGA-DSC 1, Schwerzenbach, Switzerland), about 5 mg of the sample within an alumina pan was heated from 30 °C to 600 °C at a rate of 10 °C min^{-1} in nitrogen flow, 70 ml min^{-1}. Derivative thermogravimetry (DTG) was used to identify the temperature of maximum mass-loss rates.

Differential Scanning Calorimetry (DSC) was carried out with a DSC calorimeter (Mettler Toledo 821e, Schwerzenbach, Switzerland) calibrated by an indium standard. The calorimeter cell was flushed with 100 ml min^{-1} nitrogen. The run was performed from 30 °C to 500 °C, at the heating rate of 10 °C min^{-1} and the mass sample was about 5 mg. The data processing was conducted with STARe Software.

Fourier transformed infrared (FTIR) analysis was carried out using the attenuated total reflection (ATR) technique in the range from 4000 to 650 cm^{-1} with 32 scansions and 4 cm^{-1} of band resolution by means of a Thermo Nicolet iZ10 spectrometer (Thermo Fisher Scientific, Waltham, MA, USA) equipped with a Smart EnduranceTM (ZnSe crystal) apparatus and the OMNIC 9 software.

Electrical measurements were performed on PPy-coated fabric samples cut in squares of 1 cm × 1 cm at 20 °C and 65% RH by means of a digital multimeter Escort 170 used in resistance mode and connected with two pins by each side in both weft and warp directions.

3. Results and discussion

3.1. Initial biodegradation assessment

Biodegradation behavior is well illustrated by photographs in figure 1 of samples taken from compost soil after 10 days, 30 days and 90 days.

First, among all the samples, only the untreated cotton buried in non-sterile compost soil, after 90 days, had been completely degraded, being no longer identifiable in the soil matrix (figure 1(C)).

Comparing figures 1(A) and (D), it can be noticed that the untreated cotton buried in non-sterile compost soil had become yellow-gray stained as a result of a preliminary degradation, whereas the same sample (figure 1(D)) taken after 10 days from the sterilized compost soil had maintained the natural white color of the fiber. After 30 days of burial, sample B was completely covered with soil (figure 1(B)), while 90 days were needed to observe a fabric's break into small pieces for the cotton buried in sterilized compost soil (figure 1(F)).

Instead, both after 10 days and after 30 days, no PPy-treated cotton fabrics had been degraded.

Regardless of the type of compost soil considered, sterilized or non-sterile, none of the PPy-treated samples taken from the medium, even after 90 days, suffered a macroscopic degradation, as already seen for other finished fabrics [5].

The compost-enriched soil containing sample F did not remain completely sterile until the 90th day; in fact, at about the 84th day, the presence of mold was observed. This event may have been caused by the prolonged exposition to a non-sterile laboratory environment.

Regarding the weight variations after the burial period, it is worth noticing that bare cotton samples showed the highest level of mass loss, as measured for samples B and F, which lost, respectively, 30 and 46% of their initial weight.
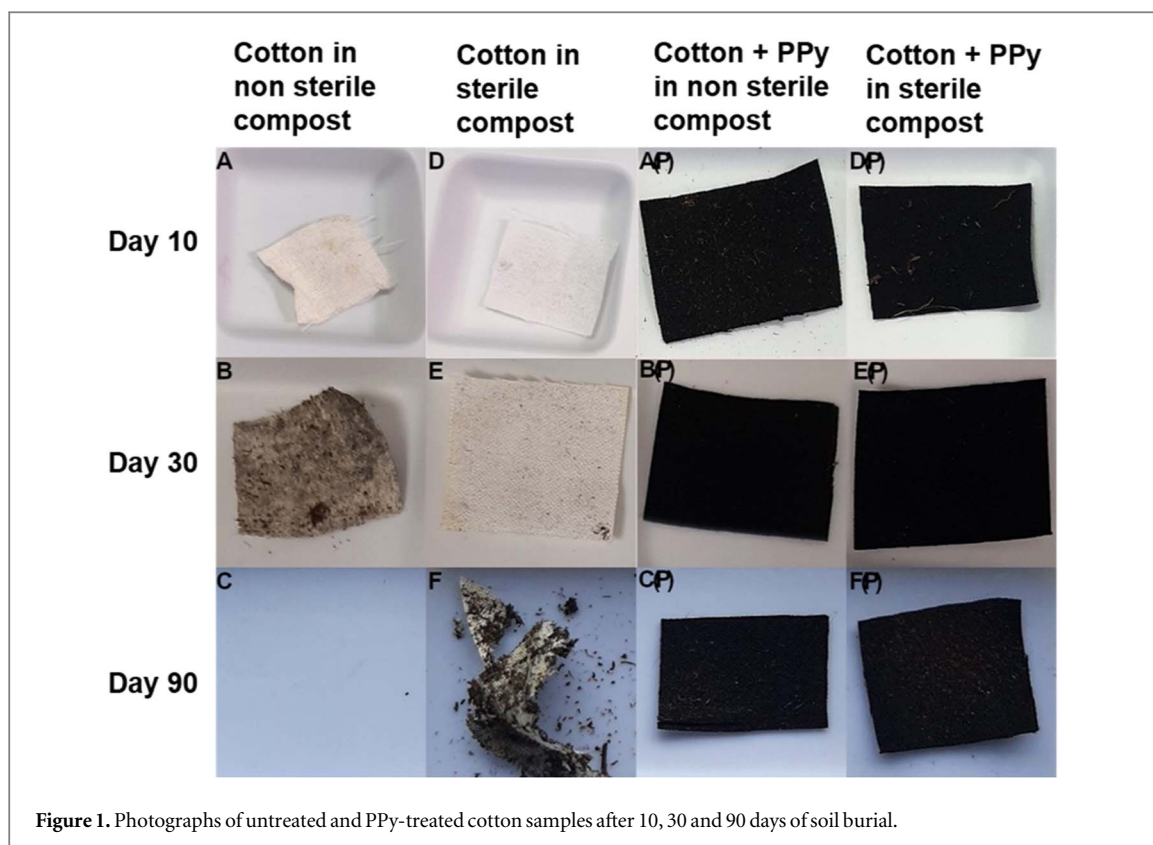
Figure 1. Photographs of untreated and PPy-treated cotton samples after 10, 30 and 90 days of soil burial.

In the case of PPy-treated samples, they showed non-significant or slight weight losses, reaching a maximum of 7%. From a purely gravimetric comparison with other works in the literature, the present result demonstrated an important stability of the PPy coating on cotton, whereas, for instance, in the paper of Benhalima *et al* [49], hydrogels based on alginate and gelatin, despite of the addition of polypyrrole, were almost entirely biodegraded after six months. Zare *et al* [42] reported that the degradation level of polypyrrole/dextrin composites was up to 74.5% in two months for the samples with low PPy:dextrin ratio, whereas for a higher presence of polypyrrole, the material after burial remained intact. According to Bideau *et al* [50], films composed of TEMPO-oxidized nanofibrillated cellulose/PPy, after 100 days of being buried, exhibited degradation of 38% (compared to the 53% of films without PPy). Such an overview gives us the possibility to realize that a remarkable influence on the biodegradation behaviors of PPy-based materials is imputable to the amount of polypyrrole, the composition of the matrix in which it is included and, plausibly, also the nature of the blend (2-D coating, bulk mixture, etc) that can influence the exposure to biotic and abiotic agents [51].

3.2. Analysis of surface morphology (SEM)

A more accurate picture of the biodegradation process was obtained by SEM analysis. Figure 2 shows the scanning electron microscope images of the untreated cotton and PPy 4 g L^{-1} treated cotton fabrics after different stages of biodegradation.

Micrographs of Cotton and Cotton-PPy are used as references. In the case of Cotton-PPy, polypyrrole was entrapped in the fabric structure, but not uniformly distributed (green arrow). Considering the untreated cotton fabrics buried in non-sterile compost-enriched soil for 30 days (B), it seems that the fibers have partially lost their initial morphology, being less linked together and creating empty spaces. The presence of extraneous particles from the soil is evident (a detail of which is reported in B*) [18, 21].

Sample C(P), PPy-treated cotton fabric after 90 days in non-sterile compost-enriched soil, showed a less damaged fiber network; still, pieces of residual soil are visible, see also C(P)*. Therefore, it was possible to verify that cotton fabrics treated with PPy followed a slower biodegradation trend than cotton fabric.

Unexpectedly, after 90 days of burial in sterilized soil, cotton sample F demonstrated the signs of microorganism presence that colonized the surface (as already anticipated by the visual inspection of mold in the beaker). On the contrary, this phenomenon was not detected in F(P), which mostly maintained its integrity, except for some minor damage. Regarding the presence of mold, it is worth recalling that it has to be correlated to the presence of fungi and these kinds of microorganisms can combine biochemical and physical actions due to their hyphal apparatus [52].
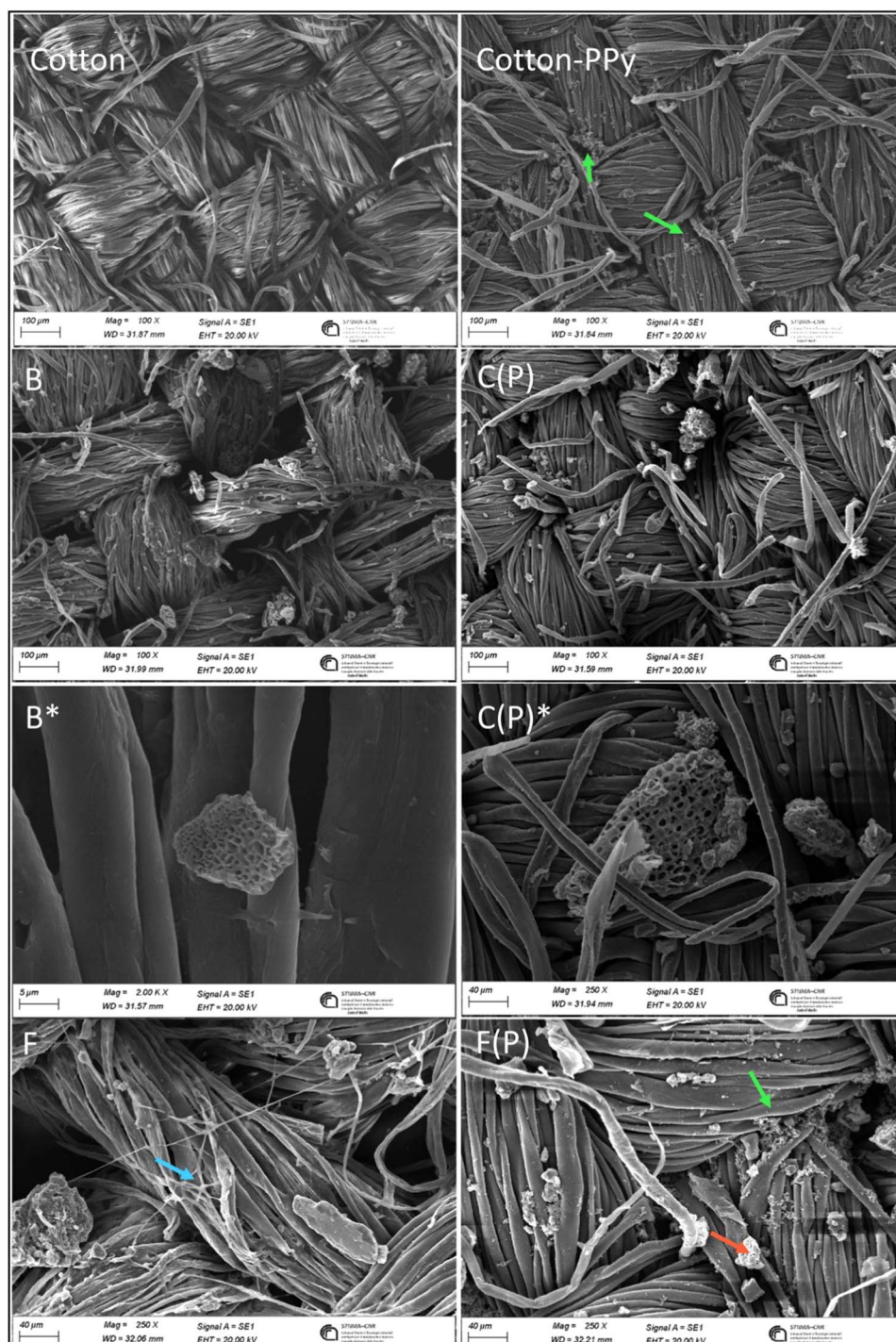
Figure 2. SEM images of the samples cotton, cotton-PPy, B, C(P), F, F(P) and details of higher magnifications B and C(P) labeled as B* and C(P)*. Green arrows indicate PPy deposition, the orange arrow points out soil residues and the light blue arrow signals the presence of mold.

3.3. Thermal analyses

DSC analyses were conducted on all the samples, a selection of which is reported in figure 3. All the events detected were endothermic. The first phenomenon (I) is generally attributed to water evaporation [53], whereas in zone III, the peak of cotton cellulose thermal degradation occurs [54] (ca. at 370 °C). More precisely, in zone III, cellulosic materials are subjected to a complex overlapping of different events, namely the fusion of their crystalline part (endothermic) and the depolymerization (exothermic) [55]. Zone II presents a peak (or a complex signal) only in the case of PPy-treated samples and, indeed, it is an index of PPy decomposition during which conjugated double bonds and polymer rings are broken (range 205 °C–315 °C) [56, 57]. In region I, the samples with polypyrrole showed a more pronounced peak, due to the overlapping of an additional event given by the PPy glass transition, as already pointed out in the literature [42, 58, 59]. Indeed, the ratio between the areas
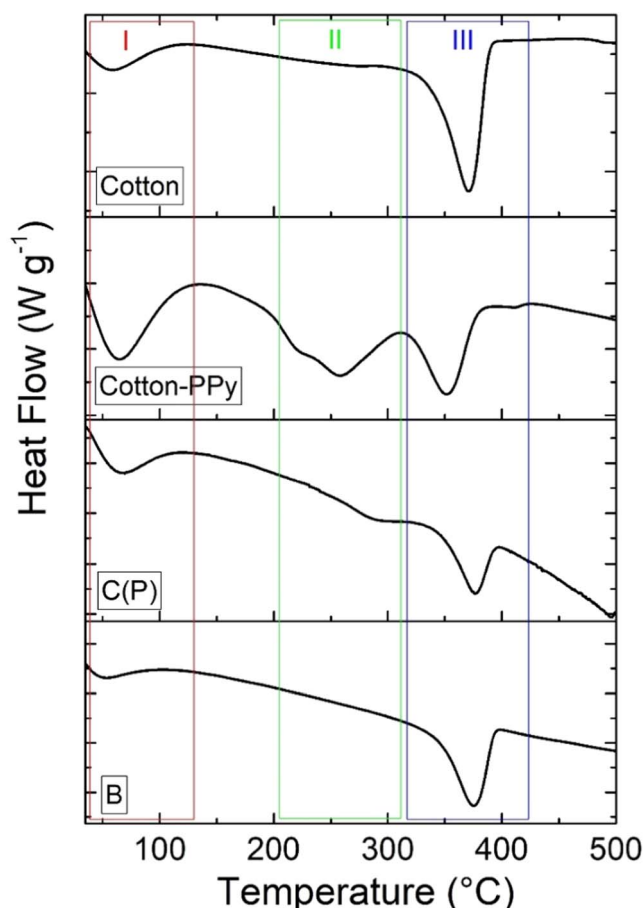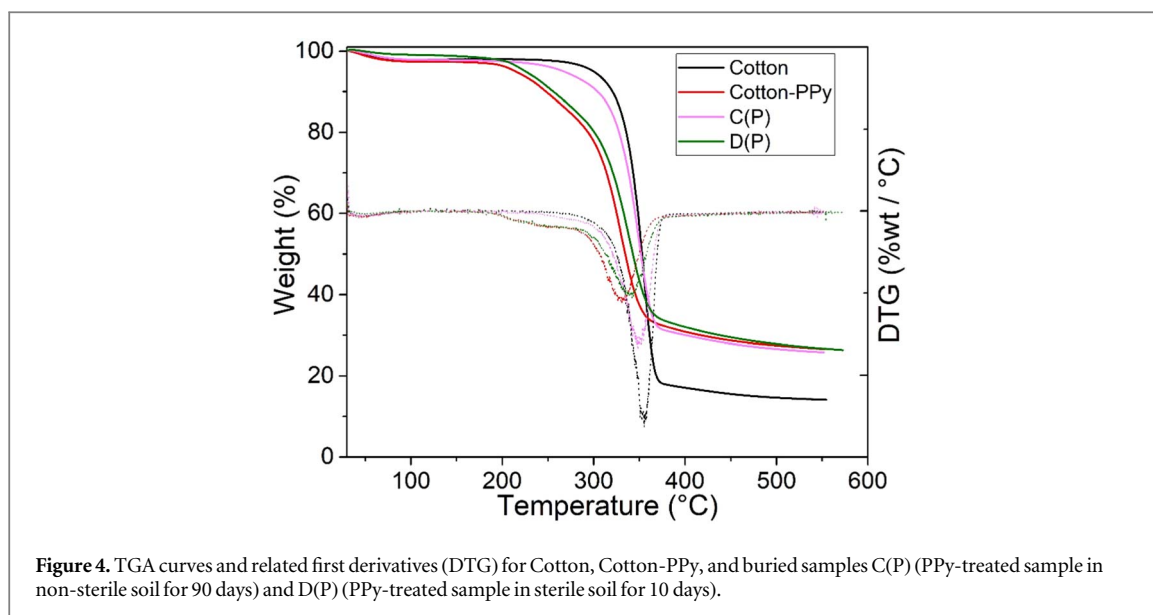
Figure 3. DSC outcomes for Cotton, Cotton-PPy, and buried samples C(P) (PPy-treated sample in non-sterile soil for three months) and B (cotton sample in non-sterile soil for one month). Zones I, II and III, comprised in the colored frames, are attributed to different thermal-induced phenomena.

subtended under the peaks of region I and region III for samples with PPy was more than doubled with respect to non-modified cotton fabrics. Another aspect to consider was the relationship between zone II and zone III. Over time, the intensity of the peak related to PPy presence (region II) became less significant and the DSC profiles more resembled that of the bare cotton. This fact is also corroborated by the temperature trend of such peaks. In the case of PPy-added samples, the peak related to cellulose decomposition (zone III) shifted at higher temperatures from 10 to 90 days, coinciding, after three months, to that of bare cotton. This trend was evident both in the case of sterilized and non-sterilized soil: it can be hypothesized, therefore, that a certain effect of the soil/moisture occurred regardless of the microorganism action and that, over time, the microbiome tended to be restored since the soil was kept in a non-sterile environment.

Regarding the enthalpies implied in the thermal events of zone II (cellulose), we could not find a trend. Indeed, even for synthetic polymers, it is not always obvious which structural parts are damaged by microorganisms. It is often thought that the amorphous regions are more susceptible to biodegradation and therefore, they are the first point of biotic attack, causing an apparent enhancement of crystallinity that can be shown by DSC [60–62]. An important criterion related to the cellulose hydrolysis rate, which is at the basis of its biodegradation, involves and is proportional to the adsorption capacity of cellulases and endoglucanases: the maximum adsorption constant of these enzymes was demonstrated to be significantly improved at low crystallinity indices [63]. Moreover, abiotic factors, such as water, are also known to exert an influence primarily on the amorphous regions of cellulose [64]. In the present work, the absence of a crystallinity trend, beyond the intrinsic issue of this determination for a semicrystalline natural macromolecule such as cotton cellulose [65], can be derived by the prolonged period in contact with microorganisms and water that could have affected both the amorphous and the crystalline portions to similar extent [66].

Thermogravimetric analyses were also carried out and some exemplifying profiles are reported in figure 4. The first observation concerned the lowest residue at 600 °C for bare cotton, whereas the behavior of the other samples mirrored the presence of the deposited polypyrrole (higher for about 12 wt%). The trend of the thermal degradation of the cotton fabric, consisting of two major stages of cleavage of glycosidic linkages followed by

Figure 4. TGA curves and related first derivatives (DTG) for Cotton, Cotton-PPy, and buried samples C(P) (PPy-treated sample in non-sterile soil for 90 days) and D(P) (PPy-treated sample in sterile soil for 10 days).

Table 2. Values of $T_{10\%}$ and $T_{50\%}$ (°C).

Parameter	Cotton	Cotton-PPy	A(P)	B(P)	C(P)	D(P)	E(P)	F(P)
$T_{10\%}$ (°C)	321	248	250	279	304	256	276	291
$T_{50\%}$ (°C)	353	335	345	347	352	343	350	358

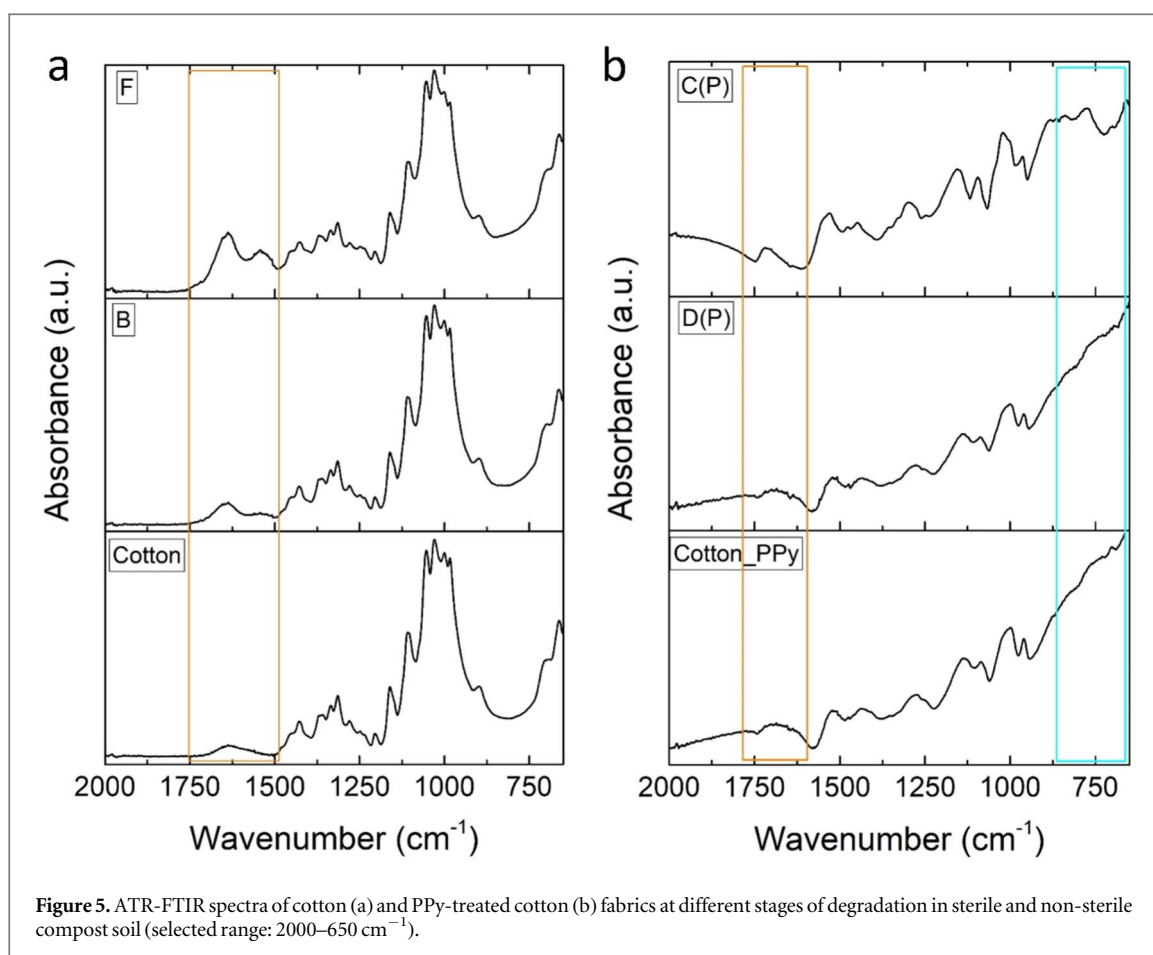dehydration and charring reactions [67], was modified after the addition of polypyrrole. Indeed, a steeper curve between 200 and 300 °C, in correspondence with both a DTG broad signal and the above-mentioned DSC peak (zone II), can be evidenced. This finding is in agreement with other studies on PPy-treated cellulose [68–70], suggesting that PPy enhances carbonizing reactions, reducing the temperature of thermal degradation. Samples C(P) and D(P), buried in very different conditions, reflected more the profile of the bare cotton and the as-prepared cotton-PPy, respectively. This way, C(P), kept for three months buried in the presence of active microorganisms, demonstrated the signs of PPy 'consumption', favoring the exposition of the cotton substrate as the principal component of the analyzed material. As a result, the buried fabrics showed again thermal degradation at higher temperatures. On the contrary, D(P), buried for only ten days in a sterilized medium, mostly maintained the original Cotton-PPy behavior. In table 2, values of $T_{10\%}$ and $T_{50\%}$ (°C) are reported: they refer to the temperatures at which the 10% and 50% weight loss is recorded, respectively. These data confirmed the progressive restoration of cotton thermal stability throughout the burial period.

3.4. ATR-FTIR characterization

Figure 5 displays the range 2000–650 cm^{-1} of some ATR-FTIR spectra, in which the vibrational features' variations were detected. The bare cotton sample signals were particularly modified between 1750 and 1500 cm^{-1}, where the small signal at 1630 cm^{-1}, related to adsorbed water [71], underwent the enhancement of its intensity and wideness and the appearance of another peak at about 1530 cm^{-1} (orange frame in figure 5(a)). This variation is progressively more intense, passing from sample B (non-sterile soil, 30 days of burial) to sample F (sterilized soil, 90 days of burial, after the emergence of mold on the soil surface). One of the reasons can lie in the presence of the degradation products of cotton. Enzymes produced by bacteria and fungi in the soil are able to catalyze the hydrolytic degradation of cellulose macromolecules, breaking of (1→4) glycosidic bonds and forming aldehyde groups, as well as the oxidative degradation of cellulose, which causes the opening of the β-d-glucopyranose rings and the formation of carboxylic and aldehyde groups [19]. Moreover, these spectral variations can be attributed to residues from microorganisms: it has already been found that these new bands, characteristic of amide groups (Amide I and Amide II), can derive from fiber-bound proteins produced by microbial growth [18, 19, 21]. Moreover, a decreased intensity of the signals centered in the zone of 1000 cm^{-1} and 1375 cm^{-1} may indicate a change from high crystalline to amorphous cellulose [19, 21].

The characteristic peaks of Cotton-PPy have been described by [34, 72]. The signals around 1525 and 1435 cm^{-1} are due to symmetric and asymmetric ring stretching modes, respectively. The band at 1525 cm^{-1} is

Figure 5. ATR-FTIR spectra of cotton (a) and PPy-treated cotton (b) fabrics at different stages of degradation in sterile and non-sterile compost soil (selected range: 2000–650 cm^{-1}).

attributed to C=C and C–N ring stretching vibrations and the band around 1275 cm^{-1} is assigned to C–H and C–N in-plane deformation modes of PPy. Furthermore, PPy has a band at about 1000 cm^{-1} corresponding to other C–H and N–H in-plane deformation vibrations, and a band at about 960 cm^{-1} assigned to C–C out-of-plane ring deformation. The spectrum showed another characteristic PPy peak at ca. 1135 cm^{-1}, which has been assigned to the bipolaronic (sulfonic groups) [42]. The peak at about 1080 cm^{-1} is ascribable to the in-plane deformation vibration of NH$^+$ groups, which are formed in the PPy chains by protonation.

In the case of the PPy-treated samples examined in this work, the only compromised specimen seemed to be C(P) (non-sterile soil, 90 days of burial). This fact is supported by the carbonyl group peak at 1720 cm^{-1}, as an index of the oxidation products or ring-opening of PPy (orange frame in figure 5(b)) [73–75]. Along the spectrum of C(P), the differences in the intensity and positions of the peaks at 1295, 1150 and 1096 cm^{-1} are also other signs of surface modifications occurring on the samples. In particular, we interpreted these spectral feature changes as the appearance of raw cotton peaks [76, 77], thus, as evidence that non-sterile soil likely erodes the PPy layer, slowly exposing cellulose again. However, the signal at 1295 cm^{-1}, accompanied by emerging small peaks at 1332 and 1355 cm^{-1}, can indicate the presence of newly formed compounds from the PPy degradation, such as *N*-(3-oxopropyl)formamide and 3-formyl-aminopropanoic acid [78], or of aminoacids derived from microorganism residues [79] (eventually covered in the region of Amide I and II by PPy bands). Moreover, in the zone of the fingerprints (light blue frame in figure 5(b)), some signals became stronger. According to the literature, that spectral region corresponds to C–H out-of-plane ring deformation and C–H rocking vibration (780 and 680 cm^{-1}) [34]. For this reason, a change in the quinoid structure of polypyrrole can be hypothesized [74, 80]. Moreover, as reported in [34, 72], the shoulder band centered at about 1020 cm^{-1} is the result of the overlaying bands attributed to functional groups of cotton cellulose, namely the C–C, C–O and C–O–C stretching vibrations. It is evident that in C(P), the intensity is higher, which is a further confirmation of the partial depletion of the PPy layer, leaving the cellulosic substrate more exposed.

3.5. Surface electrical resistivity and degradation mechanism hypothesis

The surface electrical resistivity of the PPy-coated fabric used as a reference (Cotton-PPy) was 0.45 kΩ/square in the warp direction and 0.52 kΩ/square in the weft direction. After 10 days, the resistivity increased in both directions by 3.5-fold for samples in contact with the non-sterile soil A(P) and 1.5-fold for the fabric kept in

sterilized soil D(P). After 90 days, the resistivity increment was 27–30 folds (warp) for both F(P) and C(P) (kept in sterilized and non-sterile soil, respectively), whereas, in the weft direction, C(P) was more resistive of 40 folds with respect to Cotton-PPy and 1.6 folds more resistive than F(P). These results confirmed that the PPy layer depletion was stronger in the presence of active microorganisms.

Also in light of the other characterization outcomes, these latter results can lead to hypothesizing the degradation routes. Although the persistency of the black color indicated a certain maintenance of the PPy structure, the increase in resistivity [81] (and, therefore, the reduction in conductibility) was an index of a local loss in conjugation that can be related to soil chemical and biological agents (and their synergy [62, 82]). As already discussed in [83], overoxidation processes, de-doping of the polymer and chemical attack of nucleophiles (like water molecules) can occur. Polypyrrole has also been found able to interact with organic matter, which is normally present in soil, such as humic acids, probably inducing a further alteration [84, 85]. The formation of carbonyl groups and changes in quinoid structure (see ATR-FTIR interpretation), able to interrupt the conjugation, has already been described when PPy was maintained in an air environment and in the presence of the more powerful oxidizer ozone (even causing the breaking of PPy cycle) [86–90]. Liu *et al* [91], for instance, deepened the action of humidity on conductivity: H_2O easily attacks the sites with the lower electron density, like N^+ of PPy. The initial conductivity decay was ascribed to the dopant counter-ions being expelled after the nucleophilic attack of the chemisorbed water molecules on the electroactive centers, decreasing the concentration of the positive charge carriers. The removal of counter-ions from the polymer matrix reduced the positively charged nitrogen to its neutral state, causing the conductivity to decrease. A de-doping/re-doping effect, resulting in partial conductivity losses, has also been hypothesized in the presence of inorganic species, such as chlorine anions [92], which can disrupt the conjugation when attached to the PPy chain with covalent bonds [93].

From a biological point of view, instead, both fungi and bacteria present in soil are efficient in degrading recalcitrant molecules, thanks to the production of enzymes such as mono- and di-oxygenases, dehydrogenases, laccases and hydroxylases, as already reported for N-containing heterocycles [78, 94–98]. In a recent review, studies on bacterial degradation of heterocycles, and in particular carbazole, have been reported, in which the main strains involved were *Pseudomonas*, *Sphingomonas*, *Ralstonia*, *Bacillus*, *Gordonia*, *Mycobacterium*, *Nocardioides*, *Xanthomonas*, and *Janthinobacterium* [99], which can be found in natural environments [100]. Similarly, works on different bacterial strains capable of metabolizing indole (which contain a pyrrole ring) were collected by Arora *et al* [101]. In the same review, a fungal degradation pathway of indole operated at the expense of the N-heterocyclic ring was described. The endophytic fungus *Phomopsis liquidambari* initially oxidized the indole to oxindole and isatin. Then, isatin was transformed into 2-dioxindole, which was further converted to 2-aminobenzoic acid via pyridine ring cleavage [98]. The main enzymes involved were found to be lignin peroxidase and laccase, where the latter uses molecular oxygen to oxidize various aromatic and nonaromatic compounds by a radical-catalyzed reaction mechanism [98] and are known to easily degrade nitrogen-containing structures [102]. Moreover, there is considerable evidence that pyrroles can be metabolized by cytochromes P450, as monooxygenases or multifunctional oxidases [103], which constitute a large family of heme proteins that can selectively catalyze the oxidation of a wide variety of endogenous compounds and xenobiotics including environmental pollutants [104, 105]. For instance, in Dalvie *et al* [103], it was affirmed that P450-catalyzed oxidations occur predominantly at the carbon atoms adjacent to the pyrrolyl nitrogen, generating the corresponding 3- or 4-pyrrolin-2-ones, presumably via an initial epoxide intermediate.

4. Conclusions

The degradation of PPy-finished cotton fabrics buried in compost-enriched soil was studied using a variety of characterization techniques. The degradation of the fabrics was followed over a 3-month period, with samples analyzed at regular intervals to understand the gradual changes in the fabric features.

Inspection of samples removed from the test soil after different burial times showed that the progress of the rotting process caused by microorganisms in the soil was much more intensive for the untreated than for the PPy-treated cotton samples. In particular, after 90 days of burial, the untreated cotton buried in the compost-rich soil was degraded to such an extent that it fell into unidentifiable pieces. Polypyrrole, instead, functioned as a sort of protective layer for the cotton substrate, probably due to its inherent antimicrobial characteristics; still, it has been supposed to be the first available point of attack for the action of biota and chemical agents present in the soil, since PPy progressive degradation was detected.

This work is significant since the comprehension of the biodegradation process of such materials can be helpful both in terms of the assessment of their stability performances and of their end-of-life management. As a perspective, ad hoc microbiological studies and an in-depth analysis of molecular changes in PPy can be carried out.

Acknowledgments

Not applicable.

Data availability statement

All data that support the findings of this study are included within the article (and any supplementary files).

Statements and declarations

Author contributions

All authors contributed to the study conception and design. Material preparation was performed by AV and MP; characterization was carried out by MLT and MP. The first draft of the manuscript was written by MP and MLT, and all authors revised it. All authors read and approved the final manuscript.

Funding

Declaration of interest

The authors declare that they have no known competing financial interests or personal relationships that could have appeared to influence the work reported in this paper.

Ethics approval and consent to participate

This article does not contain any studies with human participants or animals performed by any of the authors. The authors claim the compliance with the ethical standards.

Consent for publication

The authors agreed with the content and all gave explicit consent to submit and publish the results presented in the article.

ORCID iDs

Marta Piccioni ⬤ https://orcid.org/0009-0008-2908-1912
Alessio Varesano ⬤ https://orcid.org/0000-0002-5497-4842
Maria Laura Tummino ⬤ https://orcid.org/0000-0002-1869-2602

References

[1] Cuiffo M *et al* 2021 Thermochemical degradation of cotton fabric under mild conditions *Fash. Text.* **8** 25
[2] Papamichael I, Voukkali I, Economou F, Loizia P, Demetriou G, Esposito M, Naddeo V, Liscio M C, Sospiro P and Zorpas A A 2024 Mobilisation of textile waste to recover high added value products and energy for the transition to circular economy *Environ. Res.* **242** 117716
[3] Wang C *et al* 2023 A sustainable strategy to transform cotton waste into renewable cellulose fiber self-reinforcing composite paper *J. Clean. Prod.* **429** 139567
[4] Egan J and Salmon S 2021 Strategies and progress in synthetic textile fiber biodegradability *SN Appl. Sci.* **4** 22
[5] Zambrano M C, Pawlak J J and Venditti R A 2020 Effects of chemical and morphological structure on biodegradability of fibers, fabrics, and other polymeric materials *BioResources* **15** 9786

[6] Peters G, Li M and Lenzen M 2021 The need to decelerate fast fashion in a hot climate - A global sustainability perspective on the garment industry *J. Clean. Prod.* **295** 126390

[7] Agrawal R 2024 Biodegradability, sustainability, and life cycle assessment of smart textiles *Smart Text. from Nat. Resour.* (Elsevier) 273–311

[8] Muhonja C N, Makonde H, Magoma G and Imbuga M 2018 Biodegradability of polyethylene by bacteria and fungi from Dandora dumpsite Nairobi-Kenya *PLoS One* **13** e0198446

[9] Wang L, Zhang Z, Zhang D, Qiu Y, Wang Y, Quan S and Zhao L 2023 Exploring microbial degradation of polyamide 4 in soils: Unveiling degradation mechanisms, pathways, and the contribution of strain NR4 *J. Clean. Prod.* **429** 139535

[10] Al Hosni A S, Pittman J K and Robson G D 2019 Microbial degradation of four biodegradable polymers in soil and compost demonstrating polycaprolactone as an ideal compostable plastic *Waste Manag* **97** 105–14

[11] Mukherjee C, Varghese D, Krishna J S, Boominathan T, Rakeshkumar R, Dineshkumar S, Brahmananda Rao C V S and Sivaramakrishna A 2023 Recent advances in biodegradable polymers—Properties, applications and future prospects *Eur. Polym.* J **192** 112068

[12] Wang Y, van Putten R-J, Tietema A, Parsons J R and Gruter G-J M 2024 Polyester biodegradability: importance and potential for optimisation *Green Chem.* **26** 3698–716

[13] Muniyasamy S, Muniyasamy S, John M J and John M J 2017 Biodegradability of Biobased Polymeric Materials in Natural Environments *Handb. Compos. from Renew. Mater.* (Wiley) 625–53

[14] Thew C, Lee Z, Srinophakun P and Ooi C 2023 Recent advances and challenges in sustainable management of plastic waste using biodegradation approach *Bioresour. Technol.* **374** 128772

[15] Chauhan V K, Thennarasu P, Dubey R, Pandey S and Naresh R 2023 Recent efforts and advances towards sustainable ceramics made from textile wastes- a review *Open Ceram* **16** 100500

[16] Erdal N B and Hakkarainen M 2022 Degradation of cellulose derivatives in laboratory, man-made, and natural environments *Biomacromolecules* **23** 2713–29

[17] Tummino M L, Varesano A, Copani G and Vineis C 2023 A Glance at novel materials, from the textile world to environmental remediation *J. Polym. Environ.* **31** 2826–54

[18] Smith S, Ozturk M and Frey M 2021 Soil biodegradation of cotton fabrics treated with common finishes *Cellulose* **28** 4485–94

[19] Tomšič B, Simončič B, Orel B, Vilčnik A and Spreizer H 2007 Biodegradability of cellulose fabric modified by imidazolidinone *Carbohydr. Polym.* **69** 478–88

[20] Gusakov A V 2011 Alternatives to Trichoderma reesei in biofuel production *Trends Biotechnol.* **29** 419–25

[21] Arshad K, Skrifvars M, Vivod V, Valh J and Voncina B 2014 Biodegradation of natural textile materials in soil *Tekstilec.* **57** 118–32

[22] Mastalygina E E, Abushakhmanova Z R, Guyvan M Y, Brovina S D, Ovchinnikov V A and Pantyukhov P V 2022 A study of biodegradation kinetics of cellulose and its derivatives using of the sturm test *Russ. J. Appl. Chem.* **95** 1790–9

[23] Shirazi M G, Rashid A S B A, Nazir R B, Rashid A H B A, Moayedi H, Horpibulsuk S and Samingthong W 2020 Using natural limited life geotextile reinforcement - a review *Minerals* **10** 1–22

[24] Wiewel B V and Lamoree M 2016 Geotextile composition, application and ecotoxicology—a review *J. Hazard. Mater.* **317** 640–55

[25] Lawson C R 2008 Geotextile containment for hydraulic and environmental engineering *Geosynth. Int.* **15** 384–427

[26] Prambauer M, Wendeler C, Weitzenböck J and Burgstaller C 2019 Biodegradable geotextiles—an overview of existing and potential materials *Geotext. Geomembranes.* **47** 48–59

[27] Sharma N, Allardyce B, Rajkhowa R, Adholeya A and Agrawal R 2022 A substantial role of agro-textiles in agricultural applications *Front. Plant Sci.* **13** 1–11

[28] Abullah A B M 2008 https://d1wqtxts1xzle7.cloudfront.net/61066261/072_Jute_Geo-Textile20191030-63514-koep86-libre.pdf?1572430022=&response-content-disposition=inline%3B+filename%3DJute_Geo_Textiles_and_Their_Applications.pdf&Expires=1717689850&Signature=DCHVEF5ToWf63i2rVD9KLZX71rEsiYrdgd4RnwQKSMlayCLkgNbN81BOCuzT6w4d0U14dVwBbkzAMuG3tx2lLn~vw-yea9uGND5JyA6J0wi9Ny68hpS3flKrkRq6HSqfb1DHmGu4S0LQkaM6urGFX4T-FW~6sYcYrj~PmeCVWgy9Gg3jtevX7eC0JA5hMuRtGzFCx5uZoVg47bJKYy02E0X4cPsiBgxHJuN5iVU1uSOX9ndeAt8is~m~j2MDhSoNMNxOCxjVLUzi6njjS9mxO4po6Wdu7WZW0SiquwAvLZ1MlHxPtz-2nmGtmrufHwdjzBUSEHndEWXxZzazYRD8OQ__&Key-Pair-Id=APKAJLOHF5GGSLRBV4ZA

[29] Renouard S, Hano C, Ouagne P, Doussot J, Blondeau J P and Lainé E 2017 Cellulose coating and chelation of antibacterial compounds for the protection of flax yarns against natural soil degradation *Polym. Degrad. Stab.* **138** 12–7

[30] Basu G, Roy A N, Bhattacharyya S K and Ghosh S K 2009 Construction of unpaved rural road using jute-synthetic blended woven geotextile - a case study *Geotext. Geomembranes.* **27** 506–12

[31] Manna S, Saha P, Roy D, Sen R, Adhikari B and Das S 2013 Enhanced biodegradation resistance of biomodified jute fibers *Carbohydr. Polym.* **93** 597–603

[32] Pavithra S, Thejas R, Rao H N A, Krishna B S and Nagaraju G 2023 Preparation of polypyrrole by chemical oxidation: applications for sensor studies *Macromol. Res.* **32** 23-33

[33] Cabuk M, Alan Y, Yavuz M and Unal H I 2014 Synthesis, characterization and antimicrobial activity of biodegradable conducting polypyrrole-graft-chitosan copolymer *Appl. Surf. Sci.* **318** 168–75

[34] Varesano A, Aluigi A, Florio L and Fabris R 2009 Multifunctional cotton fabrics *Synth. Met.* **159** 1082–9

[35] Lu Q, Liu J, Liu Y and Zhao X 2023 Polypyrrole hollow tube/polyethylene geotextile composite for multifunctional protection prepared based on the soft template method of methyl orange *Text. Res.* J **93** 1263–73

[36] Yang Y, Liu Y and Zhao X 2022 Preparation and characterization of an electromagnetic composite polypyrrole/polyethylene short filament geotextile *Text. Res.* J **92** 1333–43

[37] Kulandaivalu S, Zainal Z and Sulaiman Y 2016 Influence of monomer concentration on the morphologies and electrochemical properties of PEDOT, PANI, and PPy prepared from aqueous solution *Int. J. Polym. Sci.* **2016** 1–12

[38] Varesano A, Belluati A, Sanchez Ramirez D O, Carletto R A, Vineis C, Tonetti C, Bianchetto Songia M and Mazzuchetti G 2016 A systematic study on the effects of doping agents on polypyrrole coating of fabrics *J. Appl. Polym. Sci.* **133** 1–9

[39] Pang A L, Arsad A and Ahmadipour M 2021 Synthesis and factor affecting on the conductivity of polypyrrole: a short review *Polym. Adv. Technol.* **32** 1428–54

[40] Ramesan M T and Suhailath K 2017 Role of nanoparticles on polymer composites *Micro Nano Fibrillar Compos. (MFCs NFCs) from Polym. Blends* (Elsevier) 301–26

[41] Sanchez Ramirez D, Varesano A, Carletto R, Vineis C, Perelshtein I, Natan M, Perkas N, Banin E and Gedanken A 2019 Antibacterial properties of polypyrrole-treated fabrics by ultrasound deposition *Mater. Sci. Eng.* C **102** 164–70

[42] Nazarzadeh Zare E, Mansour Lakouraj M and Mohseni M 2014 Biodegradable polypyrrole/dextrin conductive nanocomposite: Synthesis, characterization, antioxidant and antibacterial activity *Synth. Met.* **187** 9–16

[43] Jadoun S, Riaz U and Budhiraja V 2021 Biodegradable conducting polymeric materials for biomedical applications: a review *Med. Devices Sensors.* **4** 1–13

[44] Shustak G, Gadzinowski M, Slomkowski S, Domb A J and Mandler D 2007 A novel electrochemically synthesized biodegradable thin film of polypyrrole–polyethyleneglycol–polylactic acid nanoparticles *New J. Chem.* **31** 163–8

[45] Vahdattalab A, Khani A and Pirsa S 2023 Biodegradable cellulosic substrates modified with conductive polypyrrole nanoparticles: investigation of electrical and physicochemical properties and ability to detect temperature and humidity *J. Mater. Sci., Mater. Electron.* **34** 2036

[46] Nguyen H T, Sapp S, Wei C, Chow J K, Nguyen A, Coursen J, Luebben S, Chang E, Ross R and Schmidt C E 2014 Electric field stimulation through a biodegradable polypyrrole- co -polycaprolactone substrate enhances neural cell growth *J. Biomed. Mater. Res. Part* A **102** 2554–64

[47] Shi G, Rouabhia M, Wang Z, Dao L H and Zhang Z 2004 A novel electrically conductive and biodegradable composite made of polypyrrole nanoparticles and polylactide *Biomaterials* **25** 2477–88

[48] Rigoletto M, Calza P, Santuchi da Cunha A, Sederino V, Fabbri D, Tummino M L and Laurenti E 2023 Soybean peroxidase immobilised on cellulose-alginate hydrogels for removal of recalcitrant organic pollutants in water *React. Chem. Eng.* **8** 1629–37

[49] Benhalima T, Chicha W and Ferfera-Harrar H 2023 Sponge-like biodegradable polypyrrole-modified biopolymers for selective adsorption of basic red 46 and crystal violet dyes from single and binary component systems *Int. J. Biol. Macromol.* **253** 127532

[50] Bideau B, Bras J, Adoui N, Loranger E and Daneault C 2017 Polypyrrole/nanocellulose composite for food preservation: Barrier and antioxidant characterization *Food Packag. Shelf Life.* **12** 1–8

[51] Jafari A, Fakhri V, Kamrani S, Reza Ghaffarian Anbaran S, Su C-H, Goodarzi V, Pirouzfar V and Ali Khonakdar H 2022 Development of flexible nanocomposites based on poly(ε-caprolactone) for tissue engineering application: the contributing role of poly(glycerol succinic acid) and polypyrrole *Eur. Polym.* J **164** 110984

[52] Spina F, Tummino M L, Poli A, Prigione V, Ilieva V, Cocconcelli P, Puglisi E, Bracco P, Zanetti M and Varese G C 2021 Low density polyethylene degradation by filamentous fungi *Environ. Pollut.* **274** 116548

[53] Vyas S, Pradhan S D, Pavaskar N R and Lachke A 2004 Differential thermal and thermogravimetric analyses of bound water content in cellulosic substrates and its significance during cellulose hydrolysis by alkaline active fungal cellulases *Appl. Biochem. Biotechnol.* **118** 177–88

[54] Alharbi N D, Amer H H, El-Zaher N A and Guirguis O W 2022 Development and characterization of cotton fabrics by dipping in solutions of chitosan and ZnO-nanoparticles as promising environmentally friendly reinforcements for polymer composites *Polym. Polym. Compos.* **30** 1–12

[55] Tummino M L, Laurenti E, Bracco P, Cecone C, Parola V L, Vineis C and Testa M L 2023 Antibacterial properties of functionalized cellulose extracted from deproteinized soybean hulls *Cellulose* **30** 7805–24

[56] Rani Ananda S 2017 Thermal studies of polypyrrole and cobalt aluminum oxide nano composites *Int. J. Mater. Sci.* **12** 247–9 https://ripublication.com/ijoms17spl/ijomsv12n2spl_26.pdf

[57] Silva A, de Souza S and Sanches E 2018 Polypyrrole@ α -Al 2 O 3 and polypyrrole@CeO 2 core–shell hybrid nanocomposites *J. Compos. Mater.* **52** 1433–41

[58] Ahmad Z, Choudhary M A, Mehmood A, Wakeel R, Akhtar T and Rafiq M A 2016 Synthesis of polypyrrole nano/microspheres using cobalt(III) as an oxidizing agent and its ammonia sensing behavior *Macromol. Res.* **24** 596–601

[59] Sankar S, Parvathi K and Ramesan M T 2020 Structural characterization, electrical properties and gas sensing applications of polypyrrole/Cu-Al2O3 hybrid nanocomposites *High Perform. Polym.* **32** 719–28

[60] Eldsäter C 2000 The biodegradation of amorphous and crystalline regions in film-blown poly(ε-caprolactone) *Polymer (Guildf)* **41** 1297–304

[61] Linares Veliz A B, Jiménez J C, López P and De Gáscue B R 2019 Biodegradability study by FTIR and DSC of polymers films based on polypropylene and cassava starch *Orbital Electron. J. Chem.* **11** 71–82

[62] Silva R R A, Marques C S, Arruda T R, Teixeira S C and de Oliveira T V 2023 Biodegradation of Polymers: stages, measurement, standards and prospects *Macromol* **3** 371–39

[63] Hall M, Bansal P, Lee J H, Realff M J and Bommarius A S 2010 Cellulose crystallinity—a key predictor of the enzymatic hydrolysis rate, *FEBS* J **277** 1571–82

[64] Bertran M S and Dale B E 1986 Determination of cellulose accessibility by differential scanning calorimetry *J. Appl. Polym. Sci.* **32** 4241–53

[65] Salem K S, Kasera N K, Rahman M A, Jameel H, Habibi Y, Eichhorn S J, French A D, Pal L and Lucia L A 2023 Comparison and assessment of methods for cellulose crystallinity determination *Chem. Soc. Rev.* **52** 6417–46

[66] Gao S, You C, Renneckar S, Bao J and Zhang Y-H P 2014 New insights into enzymatic hydrolysis of heterogeneous cellulose by using carbohydrate-binding module 3 containing GFP and carbohydrate-binding module 17 containing CFP *Biotechnol. Biofuels* **7** 24

[67] Zhu P, Sui S, Wang B, Sun K and Sun G 2004 A study of pyrolysis and pyrolysis products of flame-retardant cotton fabrics by DSC, TGA, and PY–GC–MS *J. Anal. Appl. Pyrolysis* **71** 645–55

[68] Safavi-Mirmahalleh S-A, Eliseeva S N, Moghaddam A R, Roghani-Mamaqani H and Salami-Kalajahi M 2024 Synthesis and evaluation of cellulose/polypyrrole composites as polymer electrolytes for lithium-ion battery application *Int. J. Biol. Macromol.* **262** 129861

[69] Liu Z, Shang S, Chiu K, Jiang S and Dai F 2019 Fabrication of conductive and flame-retardant bifunctional cotton fabric by polymerizing pyrrole and doping phytic acid *Polym. Degrad. Stab.* **167** 277–82

[70] Yu Z, Zhu Z, Zhang Y, Li X, Liu X, Qin Y, Zheng Z, Zhang L and He H 2024 Biodegradable and flame-retardant cellulose-based wearable triboelectric nanogenerator for mechanical energy harvesting in firefighting clothing *Carbohydr. Polym.* **334** 122040

[71] Chung C, Lee M and Choe E K 2004 Characterization of cotton fabric scouring by FT-IR ATR spectroscopy *Carbohydr. Polym.* **58** 417–420

[72] Cetiner S 2014 Dielectric and morphological studies of nanostructured polypyrrole-coated cotton fabrics *Text. Res.* J **84** 1463–75

[73] Rodríguez I, Scharifker B R and Mostany J 2000 *In situ* FTIR study of redox and overoxidation processes in polypyrrole films *J. Electroanal. Chem.* **491** 117–25

[74] Mathys G I and Truong V-T 1997 Spectroscopic study of thermo-oxidative degradation of polypyrrole powder by FT-IR *Synth. Met.* **89** 103–9

[75] Chalmers E, Lee H, Zhu C and Liu X 2020 Increasing the conductivity and adhesion of polypyrrole hydrogels with electropolymerized polydopamine *Chem. Mater.* **32** 234–44

[76] Xie J, Pan W, Guo Z, Jiao S S and Ping Yang L 2019 *In situ* polymerization of polypyrrole on cotton fabrics as flexible electrothermal materials *J. Eng. Fiber. Fabr.* **14** 155892501982744

[77] Fan L, Wei C, Xu Q and Xu J 2017 Polypyrrole-coated cotton fabrics used for removal of methylene blue from aqueous solution *J. Text. Inst.* **108** 1847–52

[78] Liu H, Yang H, Yin X, Wang S, Fang S and Zhang H 2024 A novel pbd gene cluster responsible for pyrrole and pyridine ring cleavage in Rhodococcus ruber A5 *J. Hazard. Mater.* **464** 132992

[79] Barth A 2000 The infrared absorption of amino acid side chains *Prog. Biophys. Mol. Biol.* **74** 141–73

[80] Davidson R G and Turner T G 1995 An IR spectroscopic study of the electrochemical reduction of polypyrrole doped with dodecylsulfate anion *Synth. Met.* **72** 121–8

[81] Jia X, Wang C, Zhao C, Ge Y and Wallace G G 2016 Toward biodegradable Mg–Air bioelectric batteries composed of silk fibroin–polypyrrole film *Adv. Funct. Mater.* **26** 1454–62

[82] Briassoulis D and Mistriotis A 2018 Key parameters in testing biodegradation of bio-based materials in soil *Chemosphere* **207** 18–26

[83] Alumaa A, Hallik A, Sammelselg V and Tamm J 2007 On the improvement of stability of polypyrrole films in aqueous solutions *Synth. Met.* **157** 485–91

[84] Bai R and Zhang X 2001 Polypyrrole-coated granules for humic acid removal *J. Colloid Interface Sci.* **243** 52–60

[85] Laabd M, Atourki L, Chafai H, Bazzaoui M, Elamine M and Albourine A 2017 A combined experimental and DFT investigation of the adsorption of humic acid by-products on polypyrrole *J. Dispers. Sci. Technol.* **38** 1227–33

[86] Cataldo F and Omastová M 2003 On the ozone degradation of polypyrrole *Polym. Degrad. Stab.* **82** 487–95

[87] Mai T V-T, Nguyen H T and Huynh L K 2021 *Ab initio* kinetic mechanism of OH-initiated atmospheric oxidation of pyrrole *Chemosphere* **263** 127850

[88] Chen X B, Devaux J, Issi J-P and Billaud D 1994 The stability of polypyrrole electrical conductivity *Eur. Polym. J* **30** 809–11

[89] Tekle-Röttering A *et al* 2020 Reactions of pyrrole, imidazole, and pyrazole with ozone: kinetics and mechanisms *Environ. Sci. Water Res. Technol.* **6** 976–92

[90] Boutry C M, Gerber-Hörler I and Hierold C 2013 Electrically conducting biodegradable polymer composites (polylactide-polypyrrole and polycaprolactone-polypyrrole) for passive resonant circuits *Polym. Eng. Sci.* **53** 1196–208

[91] Liu Y and Hwang B 2001 Mechanism of conductivity decay of polypyrrole exposed to water and enhancement of conductivity stability of copper(I)-modified polypyrrole *J. Electroanal. Chem.* **501** 100–6

[92] Wang Z, Roberge C, Wan Y, Dao L H, Guidoin R and Zhang Z 2003 A biodegradable electrical bioconductor made of polypyrrole nanoparticle/poly(D,L-lactide) composite: A preliminary *in vitro* biostability study *J. Biomed. Mater. Res. Part* A **66A** 738–46

[93] Kaynak A 2009 Decay of electrical conductivity in p-toluene sulfonate doped polypyrrole films *Fibers Polym.* **10** 590–3

[94] Hormann K and Andreesen J 1991 A flavin-dependent oxygenase reaction initiates the degradation of pyrrole-2-carboxylate in Arthrobacter strain Py1 (DSM 6386) *Arch. Microbiol.* **157** 43–48

[95] Wang X and Xu P 2019 Microbial degradation of nitrogen heterocycles *Int. Biodeterior. Biodegradation.* **142** 170–1

[96] Fetzner S 2000 Enzymes involved in the aerobic bacterial degradation of N -heteroaromatic compounds: molybdenum hydroxylases and ring-opening 2, 4-dioxygenases *Naturwissenschaften* **87** 59–69

[97] Kamath A V and Vaidyanathan C S 1990 New pathway for the biodegradation of indole in aspergillus niger *Appl. Environ. Microbiol.* **56** 275–80

[98] Chen Y, Xie X, Ren C and Dai C 2013 Degradation of N-heterocyclic indole by a novel endophytic fungus Phomopsis liquidambari *Bioresour. Technol.* **129** 568–74

[99] Da Silva Martins L H, Rodrigues Barbosa J, Baleixo da Silva S, Portal Gomes P W, Komesu A, Vasconcelos da Silva Pereira G, Barata Alves R C and Goltara Bichara C M 2023 Microbial degradation of heterocycles- a review *J. Sci. Sustain. Eng.* **1** 1–6

[100] Ayala M, Vazquez-Duhalt R, Morales M and Le Borgne S 2017 Application of microorganisms to the processing and upgrading of crude oil and fractions *Consequences Microb. Interact. with Hydrocarb. Oils, Lipids Prod. Fuels Chem.* (Springer International Publishing) 705–40

[101] Arora P K, Sharma A and Bae H 2015 Microbial degradation of indole and its derivatives *J. Chem.* **2015** 1–13

[102] Mohamed M S M, Asair A A, Fetyan N A H and Elnagdy S M 2023 Complete biodegradation of diclofenac by new bacterial strains: postulated pathways and degrading enzymes *Microorganisms* **11** 1445

[103] Dalvie D K, Kalgutkar A S, Khojasteh-Bakht S C, Obach R S and O'Donnell J P 2002 Biotransformation reactions of five-membered aromatic heterocyclic rings *Chem. Res. Toxicol.* **15** 269–99

[104] Yang H, Yu F, Qian Z, Huang T, Peng T and Hu Z 2024 Cytochrome P450 for environmental remediation: catalytic mechanism, engineering strategies and future prospects *World J. Microbiol. Biotechnol.* **40** 33

[105] Shankar K and Mehendale H M 2014 Acetaminophen *Encycl. Toxicol.* (Elsevier) 26–9